Study of the proton 2p_{3/2}--andgt;2p_{1/2} transition in^{65}Cu and^{71}Ga

Blok, H.P.; de Jager, C.W.; de Vries, H.; de Vries, L.; Harakeh, M.N.; Heisenberg, J.H.; Heyde, K.; Riedeman, D.E.J.

published in
Physical Review C
1991

document version
Publisher's PDF, also known as Version of record

RAPID COMMUNICATIONS

PHYSICAL REVIEW C VOLUME 44, NUMBER 3 SEPTEMBER 1991

Study of the proton $2p_{3/2} \rightarrow 2p_{1/2}$ transition in ^{65}Cu and ^{71}Ga

D.E.J. Riedeman,[1] H.P. Blok,[1,2] M.N. Harakeh,[2] J.H. Heisenberg,[3] K. Heyde,[4] C.W. de Jager,[1] H. de Vries,[1] and L. de Vries[2]

[1] *National Institute for Nuclear Physics and High-Energy Physics, P.O. Box 41882, 1009 DB Amsterdam, The Netherlands*

[2] *Department of Physics and Astronomy, Vrije Universiteit, de Boelelaan 1081, 1081 HV Amsterdam, The Netherlands*

[3] *University of New Hampshire, Durham, New Hampshire 03824*

[4] *Laboratorium voor Kernfysica, Proeftuinstraat 86, B 9000 Gent, Belgium*

(Received 30 May 1991)

Electron scattering experiments on ^{65}Cu and ^{71}Ga have been performed both at forward and backward angles in order to study the transition charge and current densities of the first excited state in these nuclei. The shape and strength of these densities in ^{65}Cu as well as the strong quenching of the transition charge density in ^{71}Ga relative to that of ^{65}Cu and to single-particle estimates can be understood as resulting from pairing correlations and core polarization. The results are also supported by particle vibration coupling model calculations.

In a single-particle model the excitation from the $3/2^-$ ground state to the first excited $1/2^-$ state in the odd-A fp shell nuclei can be considered as an almost pure $2p_{3/2} \rightarrow 2p_{1/2}$ proton transition. Such a transition has already been investigated in ^{89}Y by Schwentker *et al.* [1] and by Wise *et al.* [2]. The transition charge density shows a characteristic double-humped shape, which is typical for a $2p \rightarrow 2p$ transition. However, the inner hump is strongly reduced, while the outer hump is enhanced compared to the single-particle density. These features can be explained by core polarization and pairing correlations.

According to the core polarization mechanism not only the valence nucleons play a role in a transition, but the core nucleons are also involved. The contributions of the latter may be schematically pictured as that of phonon excitations. In the transition charge density this manifests itself as an additional charge near the nuclear surface, while the inner part of the distribution is hardly affected. Therefore, there will be an increase in the transition probability $B(E\lambda)$. On the other hand, core polarization is expected to have only a small effect on the current distribution, because it is known that phonon excitations of even-even nuclei have only a small transverse part.

Due to pairing correlations, orbits above the Fermi level are partially occupied and those below this level are partially depleted. This affects the transition densities through an interference between a (forward amplitude A) transition from orbit 1 below to orbit 2 above the Fermi level and a (backward amplitude $\tilde{A}$) transition from orbit 2 to orbit 1.

In even-even nuclei [3,4] the transition from the ground state to an excited state involves mainly the creation of two quasiparticles in orbits with quantum numbers j_1 and j_2. The amplitudes $A_{\rm even}$ and $\tilde{A}_{\rm even}$ interfere constructively for the transition charge density and destructively for the transition current. In odd-A nuclei these pairing amplitudes and their interference are different [3,4]. Now, the amplitudes $A_{\rm odd}$ and $\tilde{A}_{\rm odd}$ add constructively for the transition current and destructively for the transition charge density.

While the effects of pairing correlations in even-even nuclei are well known [5], the effects in odd-A nuclei, especially the expected reduction of the transition charge density and hence also of the $B(E\lambda)$ value, have not been investigated. In this Rapid Communication the $3/2^-_1 \rightarrow 1/2^-_1$ transition is investigated in ^{65}Cu and ^{71}Ga because it is expected that pairing correlations and core polarizations have different effects in these two nuclei.

^{65}Cu and ^{89}Y are odd-A nuclei at the beginning and at the end of the fp shell, respectively. The pairing amplitudes are expected to be $A_{\rm odd} \approx 1$, $\tilde{A}_{\rm odd} \approx 0$ and $A_{\rm odd} \approx 0$, $\tilde{A}_{\rm odd} \approx 1$, respectively, so that the deviations from the single-particle transition charge and current densities due to pairing correlations should be small and mainly core polarization will affect the transition densities. However, in ^{71}Ga, which is situated in the middle of the fp shell, the forward and backward amplitudes are expected to be of the same order, resulting in a strong reduction of the transition charge density. Earlier Coulomb excitation experiments already have shown that the $B(E2)$ value for this transition in ^{71}Ga [6,7] is much smaller than that in ^{65}Cu [8].

The experiment was performed at the NIKHEF-K electron scattering facility using the high-resolution quadrupole-dipole-dipole (QDD) spectrometer [9]. For ^{65}Cu, forward scattering data were taken at scattering angles ranging from 33° to 86° covering a momentum-transfer range of $0.66 \leq q_{\rm eff} \leq 2.69$ fm^{-1} and backward scattering data at 140° in the range of $0.93 \leq q_{\rm eff} \leq 2.60$ fm^{-1}, with $q_{\rm eff} = q[1 + \frac{3}{2}(\alpha Z\hbar c/ER_{\rm eq})]$ [10]. Nine other low-q data points ($q_{\rm eff} < 0.5$ fm^{-1}) measured by Oberstedt [11] at 117°, 141°, and 165° have also been included in the data analysis. This set of electron scattering data allows to separate the transverse and longitudinal form factors. For ^{71}Ga, nine spectra at forward angles and five at a backward angle of 154° have been taken in an

effective momentum range of $1.08 \leq q_{\text{eff}} \leq 2.37$ fm^{-1} and $1.45 \leq q_{\text{eff}} \leq 2.73$ fm^{-1}, respectively.

The ^{65}Cu target was a metallic foil with an areal density of 15.4 mg/cm^2, enriched to 99.37%. For ^{71}Ga we used four pressed $^{71}Ga_2O_3$ targets strengthened by 4% CH binder and graphite with nominal thicknesses ranging from 36 to 53 mg/cm^2.

Targets of boron nitride and carbon of natural composition were used for energy calibration. A number of well-known inelastic peaks of ^{65}Cu [12] and ^{71}Ga [13] was also used in that procedure. Beam currents up till 60 μA for Cu and 25 μA for Ga have been used. The collected charge was obtained with an accuracy of 0.1% by integrating the signal from a toroid monitor. For optimum resolution the target was always set in transmission mode, except for the ^{71}Ga measurements at 154°. Because of the small dimensions of the ^{71}Ga target reflection mode had to be used at backward angles. After correction for kinematic broadening and spectrometer aberrations for ^{65}Cu a resolution of 20 to 33 keV was obtained in the forward-angle data and 40 keV for the backward-angle data. In the case of ^{71}Ga the resolution was 35 to 55 keV in the forward-angle data and 90 keV in the backward-angle data. The absolute normalization for the ^{65}Cu data was obtained from the measured target thickness plus a calibration of the detection efficiency with elastic scattering from ^{12}C [14]. The cross sections of ^{71}Ga were normalized with the aid of the elastic [15] and inelastic [16] peaks of ^{16}O observed, making use of the known chemical composition of the target.

For $3/2_1^- \rightarrow 1/2_1^-$ transitions, such as those studied in this paper, the inelastic electron scattering cross section is described by the coherent sum of the longitudinal charge form factor $C2$, the transverse electric form factor $E2$ and the transverse magnetic form factor $M1$. With unpolarized beams it is not possible to separate the $M1$ and $E2$ form factors in electron scattering experiments. The data for the transition from the $3/2_1^-$ ground state to the $1/2_1^-$ state for both nuclei have been analyzed in DWBA with the programs FOUBES1 and FOUBES2 [17].

For ^{65}Cu, the forward scattering data, which are dominated by charge scattering, were first fitted using a Fourier-Bessel expansion (FBE) [10] for the transition charge density. Subsequently, the backward scattering data for $q_{\text{eff}} < 0.5$ fm^{-1} of Ref. [11], where according to a single-particle estimate $M1$ dominates over $E2$ scattering, were fitted keeping the transition charge density fixed and adjusting the magnitude of the magnetic current density $J_{\lambda\lambda}(r)$ with its shape fixed to that for a single-particle $2p_{3/2} \rightarrow 2p_{1/2}$ transition. The single-particle wave functions used in determining the s.p. transition densities were generated in a Woods-Saxon potential with geometrical parameters r=1.25 fm, a=0.7 fm and a depth of 60 MeV which reasonably reproduces the s.p. binding energy.

Next, the $M1$ contribution to the measured cross section at higher q was subtracted assuming that the shape of the $M1$ form factor is described by that for a single-particle transition. This is a model-dependent subtraction, but at higher q the contribution of the $M1$ is nearly two orders of magnitude smaller than the $E2$ contribution (see Fig. 1). The error introduced by this assumption has been investigated by varying the single-particle $M1$ form factor for $q_{\text{eff}} > 0.5$ fm^{-1} between zero and twice its presently assumed value. This had only a small effect, especially for the transition charge density, which is determined by the longitudinal, forward-angle data. After correction for the presence of magnetic scattering $J_{\lambda\lambda}(r)$,

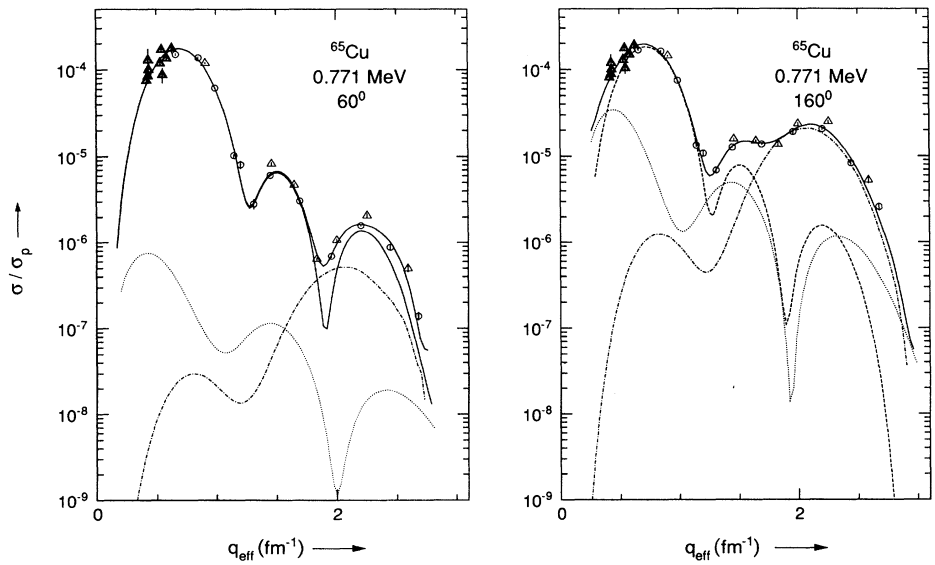

FIG. 1. Fitted form factor squared σ/σ_p versus q_{eff} for the 0.771 MeV level in ^{65}Cu. The dashed curve represents the pure charge contribution $C2$, the dotted and dot-dashed lines indicate the magnetic $M1$ and the transverse electric $E2$ contribution, respectively. The sum of $C2$, $E2$, and $M1$ is indicated by the solid curve. Forward-angle data ($\theta < 90°$) and backward-angle data ($\theta \geq 90°$), denoted by open circles and triangles in the figure, respectively, have been recalculated to 60° and 160° with the aid of the components fitted. The solid triangles are from Ref. [11].

both the charge $\rho_\lambda(r)$ and the electric term $J_{\lambda\lambda+1}(r)$ were simultaneously fitted with a FBE. A $B(E2)$ value of 96 ± 8 $e^2\text{fm}^4$ from Coulomb excitation [12] was included in the data analysis as an extra experimental data point. The resulting fits of the form factor squared, σ/σ_p, where σ_p denotes the elastic cross section for scattering from a unit point charge, are displayed in Fig. 1. In order to emphasize the contribution of the longitudinal and transverse components at forward and backward angles, σ/σ_p is shown at 60° and 160°, respectively. The recalculation of the actual data to a certain angle θ_{ref} was performed with the aid of the disentangled multipole components:

$$\sigma_{\text{exp}}(\theta_{\text{ref}}, q_{\text{eff}}) = \frac{\sigma_{\text{calc}}(\theta_{\text{ref}}, q_{\text{eff}})}{\sigma_{\text{calc}}(\theta_{\text{act}}, q_{\text{eff}})} \sigma_{\text{exp}}(\theta_{\text{act}}, q_{\text{eff}}). \quad (1)$$

Backward-angle data are indicated by triangles and the forward-angle data by circles. The solid triangles are from Ref. [11].

Unfortunately, for ^{71}Ga no low-q measurements are available. Furthermore, the presently measured cross sections are in a rather limited q-range and have large error bars. This precludes a model-independent analysis as has been performed for ^{65}Cu. In order to get a global indication of the magnitude of the charge and current densities, the shapes of the $C2$, $E2$, and $M1$ form factors were assumed to be equal to those of ^{65}Cu and only their magnitudes were varied. The measured upper limit for the $B(E2)$ value was included as an extra experimental data point with a value of 0 and an error of 1.7 $e^2\text{fm}^4$. The resulting descriptions of the data points are given in Fig. 2. As can be seen the assumption used results in an acceptable description.

By comparing the measured cross sections between ^{71}Ga and ^{65}Cu (Figs. 1 and 2) it is immediately clear that in the measured q region the charge scattering in ^{71}Ga (the forward-angle data) is at least a factor of 30 smaller than in ^{65}Cu, while the transverse cross section is much less suppressed. The extracted transition probabilities $B(E2)$ and $B(M1)$ for the 0.771 MeV transition in ^{65}Cu and the 0.390 MeV transition in ^{71}Ga are presented in Table I. The fitted value of the $B(E2)$ in ^{65}Cu is consistent with that obtained from Coulomb excitation and there is also a good agreement for the fitted $B(M1)$ value with that of Ref. [11]. The $B(E2)$ value for ^{71}Ga is strongly quenched compared to that value in ^{65}Cu, as was already evident from a direct comparison of the longitudinal cross sections. The $B(M1)$ value for ^{71}Ga has a large uncertainty as there are no transverse data points at low q. In addition a model uncertainty has to be added, which is estimated to be about 50%. The $B(M1)$ values in ^{65}Cu and ^{71}Ga seem to be of the same magnitude.

The transition charge density of ^{65}Cu presented in Fig. 3 shows a typical double-humped shape, as expected for a $2p_{3/2} \rightarrow 2p_{1/2}$ transition. Compared to the single-particle prediction the outer hump is enhanced by a factor of 2.5, which is an indication for the presence of core polarization. On the other hand the inner hump is quenched by a factor of 0.35(5), which indicates the presence of pairing correlations. The interior region of the transition current is also quenched [by a factor of 0.51(3)] as can be seen from Fig. 3, but less than the charge density.

These reduction factors can be compared with model calculations. The transition charge and current densities and the $B(E2)$ value for the $3/2_1^- \rightarrow 1/2_1^-$ transition in ^{65}Cu and ^{71}Ga were evaluated in a particle-vibration-coupling model (PVCM) [18]. In this model the transition charge and current densities are described as a sum of single-particle transitions between orbits a and b weighted by spectroscopic amplitudes $S_{ab,2}$ and a collective 2_c^+ phonon density:

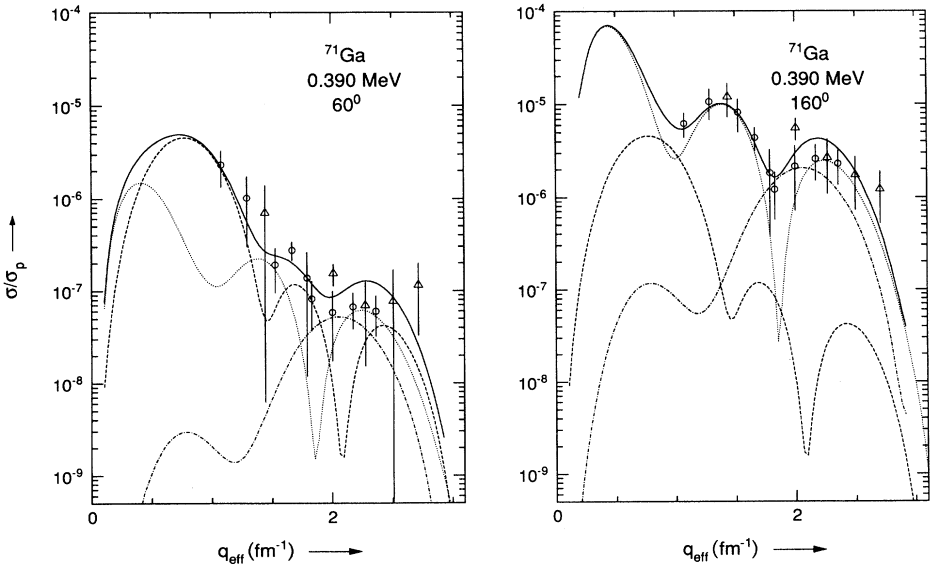

FIG. 2. Fitted form factor squared σ/σ_p for the 0.390 MeV level in ^{71}Ga. The curves are as explained in Fig. 1.

TABLE I. Transition probabilities from the ground state to the 0.771 MeV and 0.390 MeV levels in ^{65}Cu and ^{71}Ga, respectively.

	^{65}Cu		^{71}Ga	
	$B(E2)$ (e^2fm^4)	$B(M1)$ (μ_N^2)	$B(E2)$ (e^2fm^4)	$B(M1)$ (μ_N^2)
Single-particle model	28.8	1.63	34.1	1.59
PVCM	92.3	0.478	0.012	0.41
Coulomb excitation [6–8]	96.0±8.0	0.43±0.03	<1.7	
(e,e') [11]	77.0±7.0	0.31±0.03		
Present experiment	89.0±2.8	0.33±0.05	1.3±1.0	0.83±0.34

$$\rho_2(r) = \sqrt{\frac{1}{2J_f+1}} \sum_{a,b} \rho_2^{ab}(r) S^{\rho}_{ab,2} + \beta \rho_{0_c^+ \to 2_c^+}(r) \ , \qquad (2)$$

$$j_2(r) = \sqrt{\frac{1}{2J_f+1}} \sum_{a,b} j_2^{ab}(r) S^{j}_{ab,2} + \beta j_{0_c^+ \to 2_c^+}(r) \ . \qquad (3)$$

The first term in (2) and (3) denotes the single-particle contribution, while the summation a and b runs over the valence orbitals $1g_{9/2}$, $2p_{3/2}$, $2p_{1/2}$, and $1f_{5/2}$. The second term is due to the 2_c^+ phonon density, i.e., core polarization, where β is a scaling factor for the collective transition rate in the odd-A nucleus compared to that of the core even-even nucleus. The pairing factors $A - \tilde{A}$ and $A + \tilde{A}$ are included in the spectroscopic amplitudes $S^{\rho}_{ab,2}$ and $S^{j}_{ab,2}$, respectively. For both ^{65}Cu and ^{71}Ga the s.p. term for the transition in (2) and (3) is dominated by a large spectroscopic factor calculated for the $2p_{3/2} \to 2p_{1/2}$ s.p. transition. In this model the collective term in the current can be neglected, because it is known that for collective $0^+ \to 2^+$ transitions j is rather small.

The relative phase of the s.p. and collective terms in (2) and (3) depends on the difference in the energies ϵ of the s.p. orbits and the 2_c^+ phonon energy $\hbar\omega_2$ in the neighboring even-even nucleus. If $|\epsilon_{2p_{3/2}} - \epsilon_{2p_{1/2}}| < \hbar\omega_2$ there is constructive interference of the s.p. and collective matrix elements, otherwise the interference will be destructive [19].

In ^{65}Cu the s.p. matrix and collective matrix elements have the same sign since $|\epsilon_{2p_{3/2}} - \epsilon_{2p_{1/2}}|$=1.03 MeV is smaller than the phonon energy $\hbar\omega_2$=1.35 MeV in ^{64}Ni. This leads to an enhanced value for the transition strength [$B(E2)_{\rm PVCM}$=92.2 e^2fm^4] in comparison to the s.p. value. In r space this results in an enhanced peak at the nuclear surface in comparison to the double-humped s.p. $2p_{3/2} \to 2p_{1/2}$ transition charge density. In PVCM the theoretical forward and backward amplitudes for ^{65}Cu are A=1 and $\tilde{A}$=0. Experimentally, the ratio of the scale factors for the transition charge and current densities is

$$(A - \tilde{A})/(A + \tilde{A}) = 0.68 \pm 0.14 \ ,$$

which yields

$$\tilde{A}/A = 0.18 \pm 0.08 \ .$$

Unfortunately, for ^{71}Ga, the shape of the densities could not be extracted. Therefore, a one-quasiparticle calculation (including pairing) was performed in PVCM,

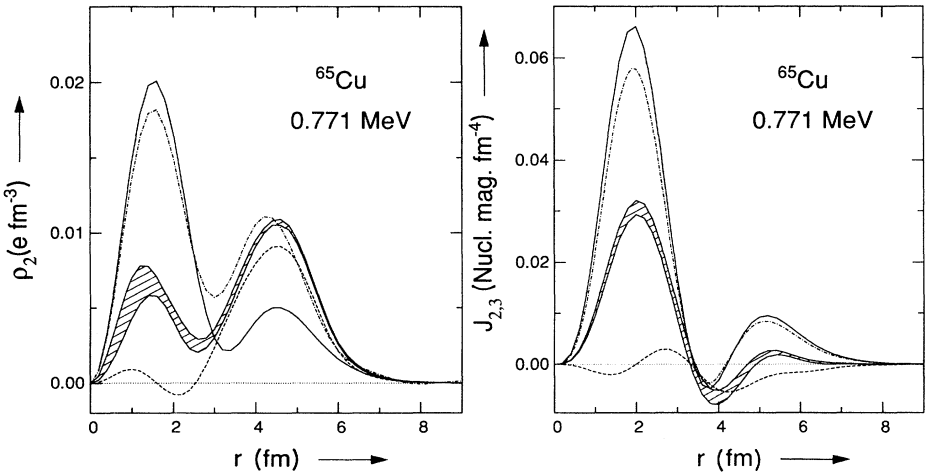

FIG. 3. The experimental transition charge densities and current densities for the $1/2_1^-$ level at 0.771 MeV in ^{65}Cu. The hatched areas show the experimental data with their errors. The solid curve indicates the single-particle prediction. Core polarization effects in ^{65}Cu are represented by the dashed lines and are similar in shape to the transition densities of the 2_1^+ state in ^{64}Ni [20]. The PVCM calculation is represented by the dot-dashed curves.

which yielded forward and backward amplitudes of 0.63 and 0.26, respectively. Two mechanisms result in a very low $B(E2)$ value in ^{71}Ga relative to ^{65}Cu. Firstly, the single-particle matrix element, which is dominated by the $2p_{3/2} \rightarrow 2p_{1/2}$ transition is quenched because of the pairing factor $A - \tilde{A}$=0.37. Secondly, the s.p. and collective matrix elements now have opposite signs since $|\epsilon_{2p_{3/2}} - \epsilon_{2p_{1/2}}|$=1.33 MeV is larger than the phonon energy $\hbar\omega_2$=0.88 MeV in ^{70}Zn. Hence, the 2_c^+ phonon density and $2p_{3/2} \rightarrow 2p_{1/2}$ s.p. transition charge density almost cancel at the nuclear surface. The two effects lead to a very small $B(E2)$ value of 0.012 e^2fm^4. Experimentally, one finds a value of 1.3 ± 1.0 e^2fm^4, in rather good agreement with the theoretical value.

Summarizing, we have measured longitudinal and transverse cross sections for the $3/2_1^- \rightarrow 1/2_1^-$ transition in ^{65}Cu and ^{71}Ga which in a single-particle model can be considered as a pure $2p_{3/2} \rightarrow 2p_{1/2}$ proton transition. The effects of core polarization and pairing correlations in ^{65}Cu are similar to those in ^{89}Y. Pairing correlations reduce the transition charge density in the nuclear interior while core polarization strongly enhances it in the nuclear surface region. For ^{71}Ga the longitudinal form factor is strongly quenched as is also reflected in the small $B(E2)$ value, which is nearly two orders of magnitude smaller than in ^{65}Cu. This is due to a cancellation between the collective transition charge density resulting from core polarization and the s.p. transition charge density that is already quenched by pairing correlations. On the other hand, the transverse form factors for both nuclei are comparable.

The authors would like to thank A. Oberstedt for supplying the low-q data prior to publication and K. Allaart for useful discussions. Further acknowledgments go to W. Lozowski (IUCF) and K. Wiederspahn for supplying the gallium and copper targets, respectively. This work was part of the research program of the Nationaal Instituut voor Kernfysica en Hoge Energie Fysica (NIKHEF, sectie K) and Stichting voor Fundamenteel Onderzoek der Materie (FOM), which is financially supported by the Nederlandse Organisatie voor Wetenschappelijk Onderzoek (NWO), and of the National Science Foundation's U.S.–Netherlands Cooperative Research Project No. 8619753.

[1] O. Schwentker, J. Dawson, J. Robb, J. Heisenberg, J. Lichtenstadt, C.N. Papanicolas, J. Wise, J.S. McCarthy, L.T. van der Bijl, and H.P. Blok, Phys. Rev. Lett. **50**, 15 (1983).

[2] J.E. Wise, F.W. Hersman, J.H. Heisenberg, T.E. Milliman, J.P. Connelly, J.R. Calarco, and C.N. Papanicolas, Phys. Rev. C **42**, 1077 (1990).

[3] D.J. Rowe, *Nuclear Collective Motion* (Methuen, London, 1970), p. 200.

[4] K. Allaart, E. Boeker, G. Bonsignori, M. Savoia, and Y.K. Gambhir, Phys. Rep. **169**, 209 (1988).

[5] O. Schwentker, J. Dawson, S. McCaffrey, J. Robb, J. Heisenberg, J. Lichtenstadt, C.N. Papanicolas, J. Wise, J.S. McCarthy, N. Hintz, and H.P. Blok, Phys. Lett. **112B**, 40 (1982).

[6] D.S. Andreev, A.P. Grinberg, G.M. Gusinskii, K.I. Erokhina, V.S. Zvonov, and I. Kh. Lemberg, Izv. Akad. Nauk SSSR, Ser. Fiz. **36**, 818 (1972); Bull. Acad. Sci. USSR, Phys. Ser. **36**, 738 (1973).

[7] M. Ivaşcu, D. Bucurescu, D. Popescu, V. Avrigeanu, E. Drăgulescu, G. Semenescu, and M. Avrigeanu, Nucl. Phys. **A225**, 357 (1974).

[8] R.L. Robinson and Z.W. Grabowski, Nucl. Phys. **A191**, 225 (1972).

[9] C. de Vries, C.W. de Jager, L. Lapikás, G. Luijckx, R. Maas, H. de Vries, and P.K.A. de Witt Huberts, Nucl. Instrum. Methods **223**, 1 (1984).

[10] J. Heisenberg and H.P. Blok, Annu. Rev. Nucl. Part. Sci. **33**, 569 (1983).

[11] A. Oberstedt, Diplomarbeit, Darmstadt, 1986, unpublished.

[12] N.J. Ward and J.K. Tuli, Nucl. Data Sheets **47**, 1 (1986).

[13] M.R. Bhat and D.E. Alburger, Nucl. Data Sheets **53**, 1 (1988).

[14] H. de Vries, C.W. de Jager, and C. de Vries, At. Data Nucl. Data Tables **36**, 495 (1987).

[15] G. Lahm, Ph.D. thesis, University of Mainz, 1982 (unpublished) and private communication.

[16] T.N. Buti *et al.*, Phys. Rev. C **33**, 755 (1986).

[17] J. Heisenberg, *Advances in Nuclear Physics,* edited by J.W. Negele and E. Vogt (Plenum, New York, 1981), Vol. 12.

[18] K. Heyde and P.J. Brussaard, Nucl. Phys. **A104**, 81 (1967).

[19] K. Heyde, M. Waroquier, and H. Vincx, Phys. Lett. **57B**, 429 (1975).

[20] A. Yokoyama and K. Ogawa, Phys. Rev. C **39**, 2458 (1989).